26. Star forming activity in the H II regions associated with IRAS 17160-3707 complex

G. Nandakumar, V. S. Veena, S. Vig, A. Tej, S. K. Ghosh and D. K. Ojha （AJ）

We present a multiwavelength investigation of star formation activity towards the southern H II regions associated with IRAS 17160–3707, located at a distance of 6.2 kpc with a bolometric luminosity of $8.3 \times 10^5 \, L_\odot$. The ionised gas distribution and dust clumps in the parental molecular cloud are examined in detail using measurements at infrared, submillimeter and radio wavelengths. The radio continuum images at 1280 and 610 MHz obtained using Giant Metrewave Radio Telescope reveal the presence of multiple compact sources as well as nebulous emission. At submillimeter wavelengths, we identify seven dust clumps and estimate their physical properties like temperature: $24 - 30 \, \mathrm{K}$, mass: $300 - 4800 \, M_\odot$ and luminosity: $9 - 317 \times 10^2 \, L_\odot$ using modified blackbody fits to the spectral energy distributions between 70 and 870 μm. We find 24 young stellar objects in the mid-infrared, with few of them coincident with the compact radio sources. The spectral energy distributions of young stellar objects have been fitted by the Robitaille models and the results indicate that those having radio compact sources as counterparts host massive objects in early evolutionary stages with best fit age $\leq 0.2 \, \mathrm{Myr}$. We compare the relative evolutionary stages of clumps using various signposts such as masers, ionised gas, presence of young stellar objects and infrared nebulosity and find six massive star forming clumps and one quiescent clump. Of the former, five are in a relatively advanced stage and one in an earlier stage.

Candidate Water Vapor Lines to Locate the H2O Snowline through High-Dispersion Spectroscopic Observations I. The Case of a T Tauri Star

Shota Notsu, Hideko Nomura, et al (ApJ in press)

Inside the H_2O snowline of protoplanetary disks, water evaporates from the dust-grain surface into the gas phase, whereas it is frozen out on to the dust in the cold region beyond the snowline. H_2O ice enhances the solid material in the cold outer part of a disk, which promotes the formation of gas-giant planet cores. We can regard the H_2O snowline as the surface that divides the regions between rocky and gaseous giant planet formation. Thus observationally measuring the location of the H_2O snowline is crucial for understanding the planetesimal and planet formation processes, and the origin of water on Earth. In this paper, we find candidate water lines to locate the H_2O snowline through future high-dispersion spectroscopic observations. First, we calculate the chemical composition of the disk and investigate the abundance distributions of H_2O gas and ice, and the position of the H_2O snowline. We confirm that the abundance of H_2O gas is high not only in the hot midplane region inside the H_2O snowline but also in the hot surface layer of the outer disk. Second, we calculate the H_2O line profiles and identify those H_2O lines which are promising for locating the H_2O snowline: the identified lines are those which have small Einstein A coefficients and high upper state energies. The wavelengths of the candidate H_2O lines range from mid-infrared to sub-millimeter, and they overlap with the regions accessible to ALMA and future mid-infrared high dispersion spectrographs (e.g., TMT/MICHI, SPICA).
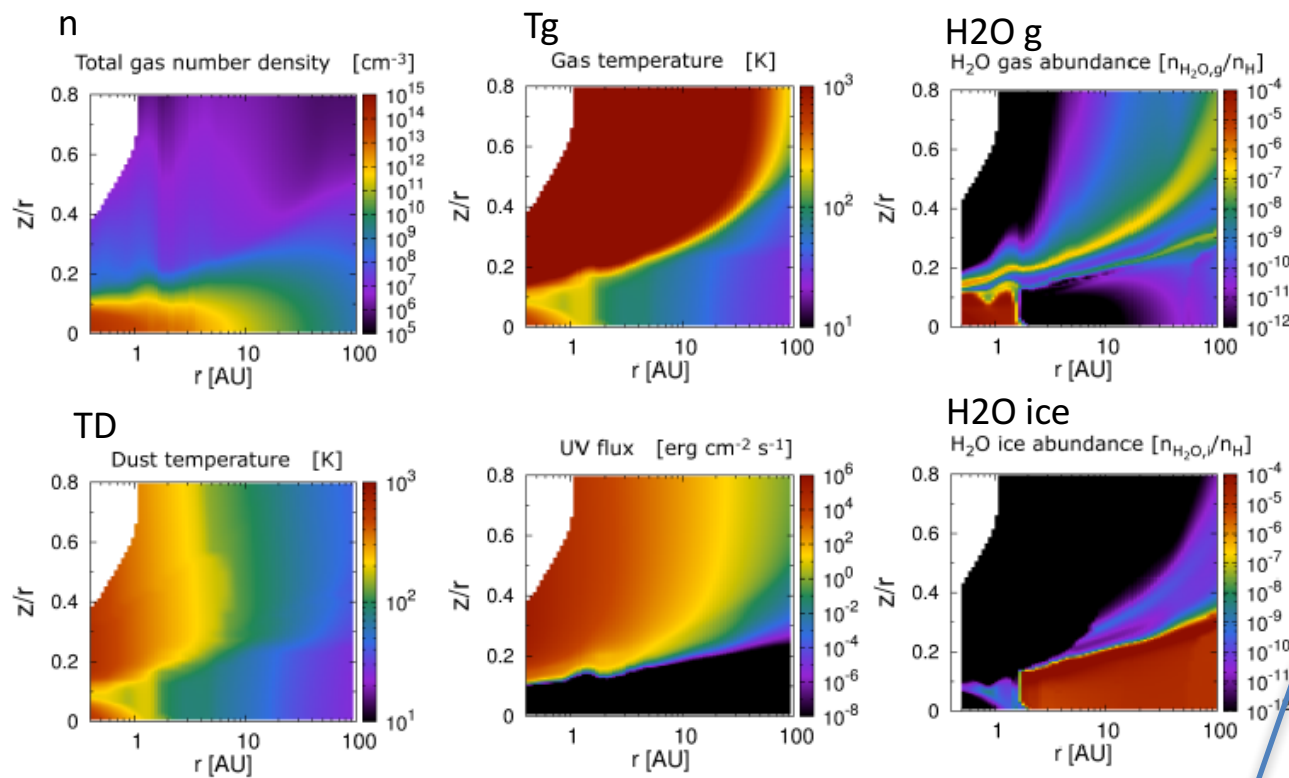
H2O snowlineを観測的に決める意義。
（1）Snowline 外では、H2Oマントルがダストの付着成長を促進 --> ガス惑星のコア。
（2）地球型惑星の水の量を決定。
将来のH2O分光観測からH2O snowlineを観測的に決める試み。

A係数が適当に小さく、E~1000K位の高い遷移を選択すること。

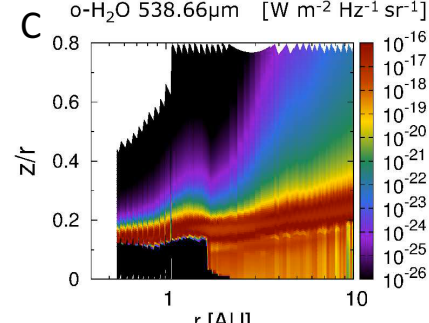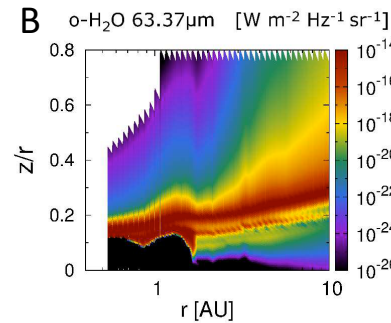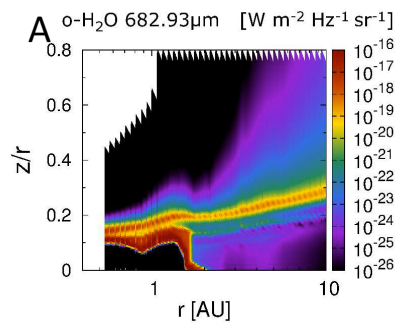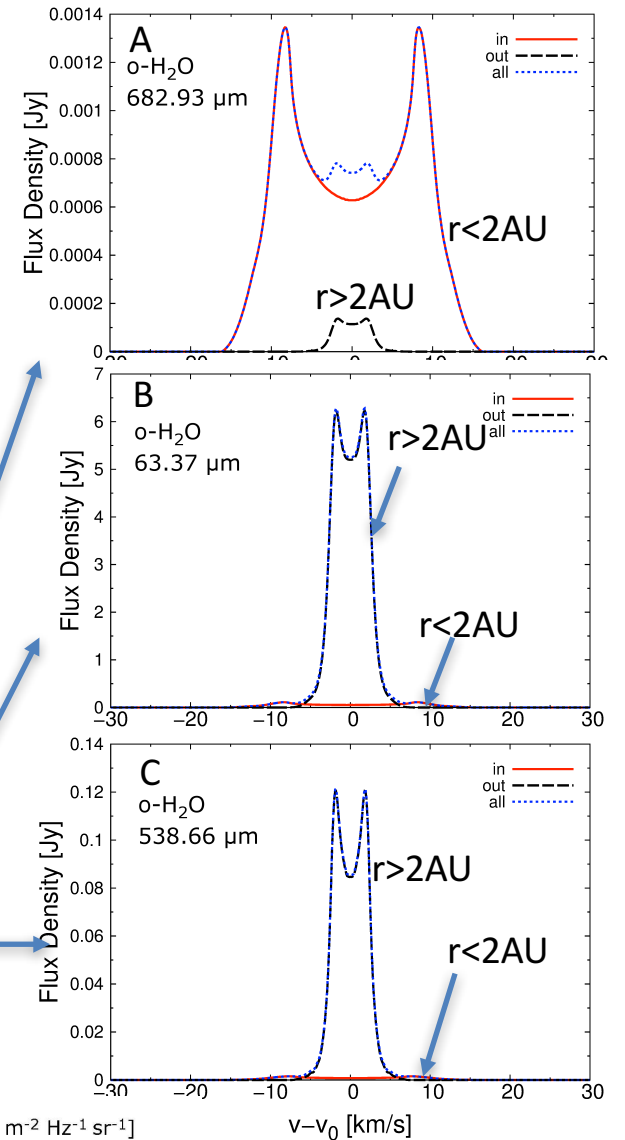**n** — Total gas number density [cm^{-3}]

Tg — Gas temperature [K]

H2O g — H_2O gas abundance [$n_{H_2O,g}/n_H$]

TD — Dust temperature [K]

UV flux [erg cm^{-2} s^{-1}]

H2O ice — H_2O ice abundance [$n_{H_2O,i}/n_H$]

A — o-H_2O 682.93 μm — r<2AU, r>2AU

B — o-H_2O 63.37 μm — r>2AU, r<2AU

C — o-H_2O 538.66 μm — r>2AU, r<2AU

$J_{K_a K_c}$	λ	Freq.	A_{ul}	E_{up}	n_{cr}	total flux[1]
	[μm]	[GHz]	[s^{-1}]	[K]	[cm^{-3}]	[W m^{-2}]
A	$6_{43}-5_{50}$	682.926	439.286	2.816×10^{-5}	1088.7	1.0×10^{6}	3.12×10^{-22}
B	$8_{18}-7_{07}$	63.371	4733.995	1.772	1070.6	1.5×10^{10}	5.66×10^{-18}
C	$1_{10}-1_{01}$	538.664	556.933	3.497×10^{-3}	61.0	2.9×10^{7}	1.13×10^{-20}

Note: column alignment — A row: $6_{43}-5_{50}$ under $J_{K_aK_c}$, 682.926 under λ, 439.286 under Freq., 2.816×10^{-5} under A_{ul}, 1088.7 under E_{up}, 1.0×10^{6} under n_{cr}, 3.12×10^{-22} under total flux.

[1] In calculating total flux of these H_2O lines, we use a distance $d = 140$pc and the inclination angle of the disk $i = 30$ deg.

H2O snowline内の光学的に厚いディスク起源、2つのピーク内側構造が
雪線のケプラー速度に対応する。

A o-H_2O 682.93μm [W m^{-2} Hz^{-1} sr^{-1}]

B o-H_2O 63.37μm [W m^{-2} Hz^{-1} sr^{-1}]

C o-H_2O 538.66μm [W m^{-2} Hz^{-1} sr^{-1}]

B.雪線内外のディスク表面

C.雪線内外のディスク表面
雪線外のディスクも寄与

A Wide-Field Survey for Transiting Hot Jupiters and Eclipsing Pre-Main-Sequence Binaries in Young Stellar Associations, Ryan J. Oelkers, Lucas M. Macri et al (AJ)

The past two decades have seen a significant advancement in the detection, classification and understanding of exoplanets and binaries. This is due, in large part, to the increase in use of small-aperture telescopes (< 20 cm) to survey large areas of the sky to milli-mag precision with rapid cadence. The vast majority of the planetary and binary systems studied to date consist of main-sequence or evolved objects, leading to a dearth of knowledge of properties at early times (<50 Myr). Only a dozen binaries and one candidate transiting Hot Jupiter are known among pre-main sequence objects, yet these are the systems that can provide the best constraints on stellar formation and planetary migration models. The deficiency in the number of well-characterized systems is driven by the inherent and aperiodic variability found in pre-main-sequence objects, which can mask and mimic eclipse signals. Hence, a dramatic increase in the number of young systems with high-quality observations is highly desirable to guide further theoretical developments. We have recently completed a photometric survey of 3 nearby (<150 pc) and young (<50 Myr) moving groups with a small aperture telescope. While our survey reached the requisite photometric precision, the temporal coverage was insufficient to detect Hot Jupiters. Nevertheless, we discovered 346 pre-main-sequence binary candidates, including 74 high-priority objects for further study.
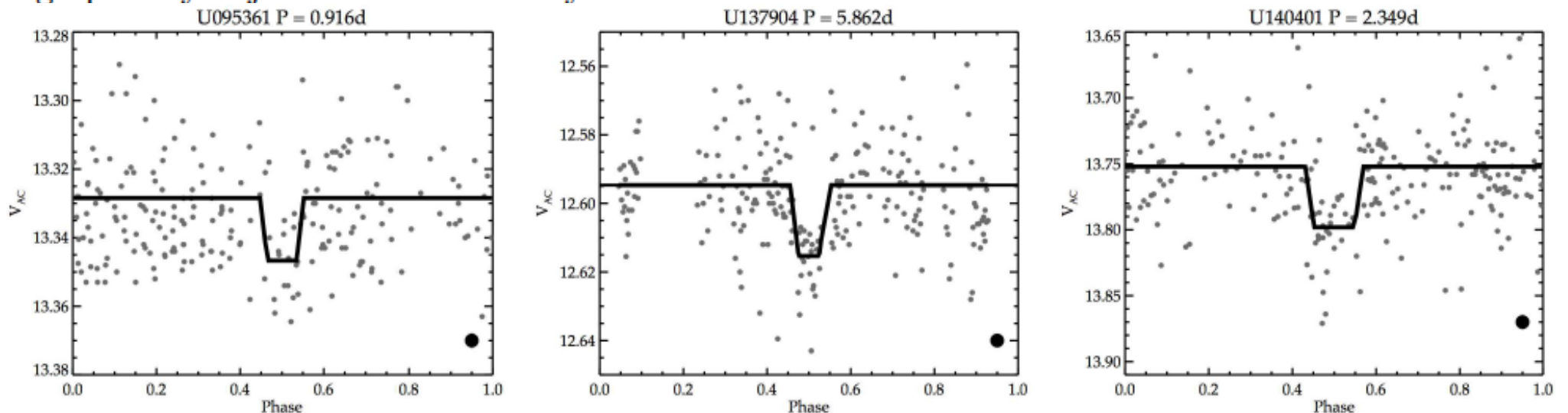
（上図）7個のPMS周りのhot Jupitor候補見つかる。しかしFollow-up精密測光観測ではtransitの証拠なし。

A Dwarf Transitional Protoplanetary Disk around XZ Tau B
Mayra Osorio, Enrique Macias, et al (ApJL)

We report the discovery of a dwarf protoplanetary disk around the star XZ Tau B that shows all the features of a classical transitional disk but on a much smaller scale. The disk has been imaged with the Atacama Large Millimeter/Submillimeter Array (ALMA), revealing that its dust emission has a quite small radius of ∼3.4 au and presents a central cavity of ∼1.3 au in radius that we attribute to clearing by a compact system of orbiting (proto)planets. Given the very small radii involved, evolution is expected to be much faster in this disk (observable changes in a few months) than in classical disks (observable changes requiring decades) and easy to monitor with observations in the near future. From our modeling we estimate that the mass of the disk is large enough to form a compact planetary system.

Transitional disk: 中心cavity, 空隙をもつディスク、
R~50-100AU, M~10-100MJ, Rcav~15-70AU
小さいTransitional diskの存在：SEDでは予測されていた。
直接撮像: R~3.4AU, Rcav~1.3AU

Zapata+2015
ALMASci.Verification

バブル
A/C起源

CO(1-0)
8.25~10.75km/s

XZ Tau 3重星
A-C sep~0."09sec
A/C − B sep.~0."3

CO(1-0)
0.75~4.5km/s

Blue/Red Contours: CO(1–0)
White Contours: 3mm
Grey Scale: optical
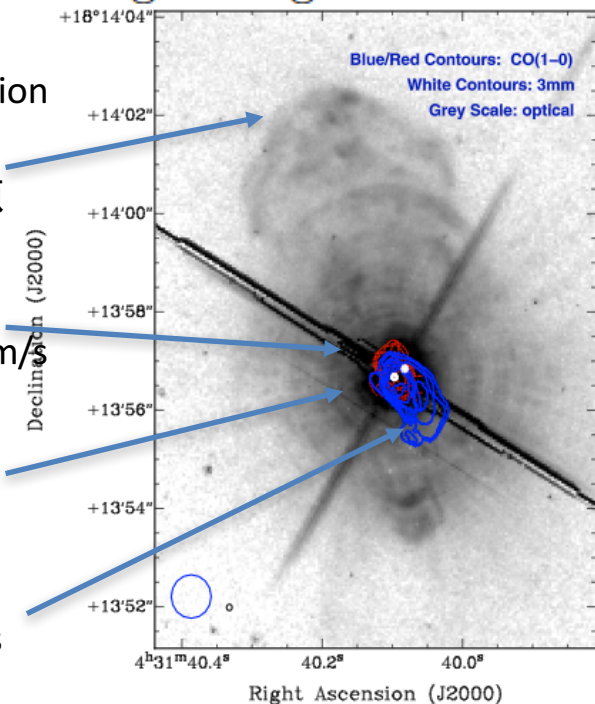
Long baseline campaign of ALMA 2.9mm, 1.3mm
2.9mm → unresolved
1.3mm → angularly resolve

Irradiated α降着円盤モデル(D'Alessio 2006)

α=0.001

α=0.01

$M_p=0.12\ M_J,\ a=1e-3$
0, 1e4, 5e4, 1e5 yrs

t=0
10^4
5 10^4

ガス

10^5

ダスト

$M_p=0.12\ M_J,\ \alpha=0.01$
0, 1e4, 5e4, 7.4e4 yrs

10^4

t=0

5 10^4

ガス

7.4 10^4
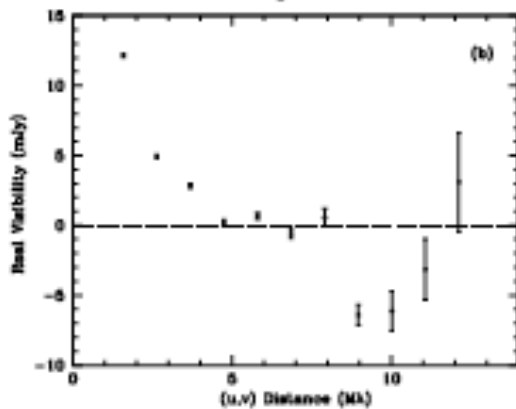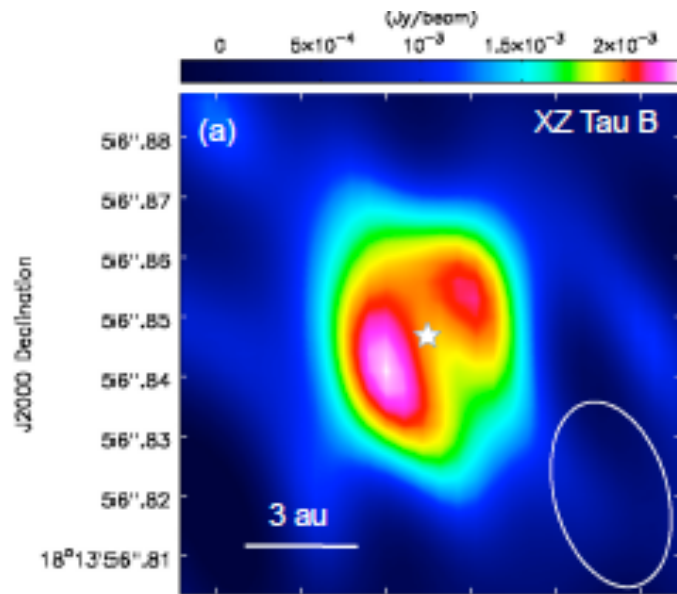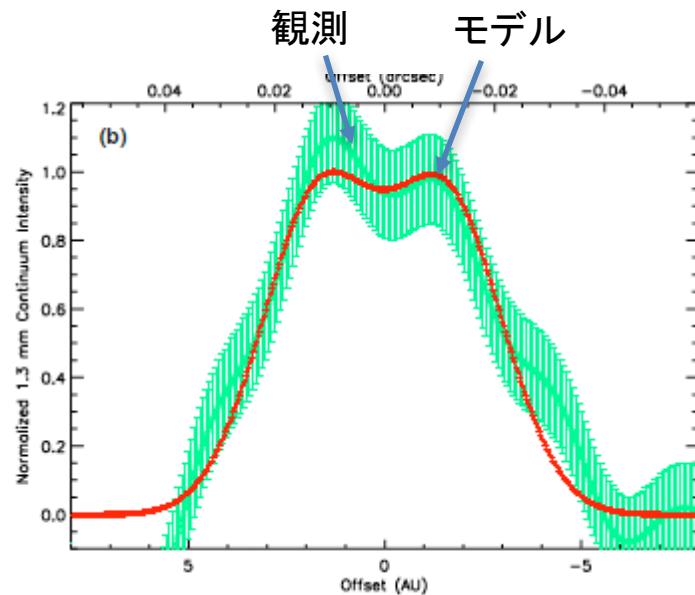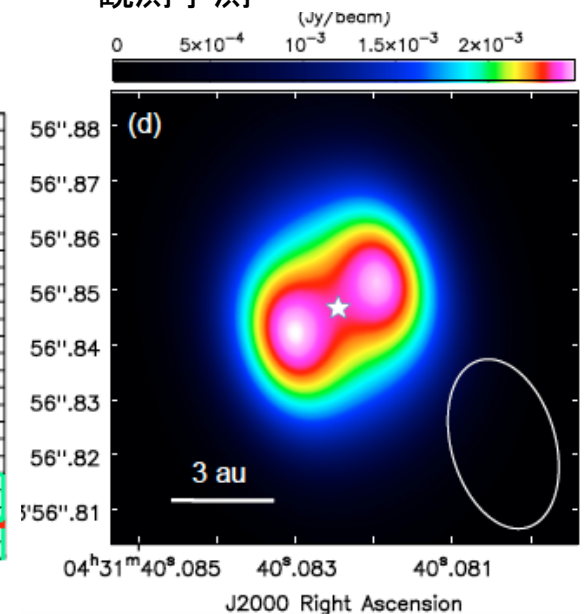
ダスト

$\log_{10}\Sigma(g\ cm^{-2})$

R (AU)
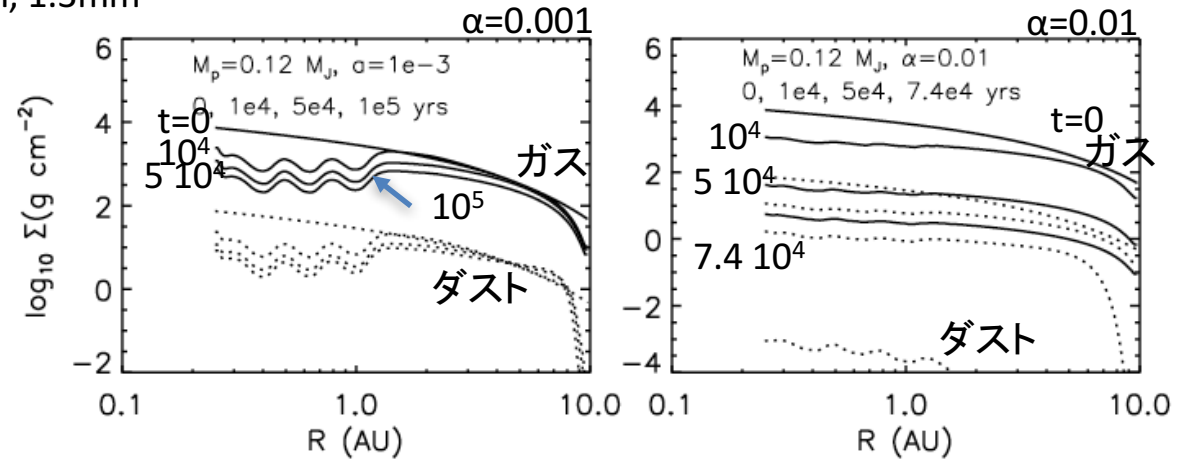
Fig. 2.— Hydrodynamical simulations of the surface density (solid line=gas; dotted line=1 mm dust) at different times for viscous disks (α=0.001, left; α=0.01, right) with three accreting 0.12 M_J planets, at radii 0.4, 0.63, and 1 au.

(Jy/beam)
0   5×10^{-4} 10^{-3} 1.5×10^{-3} 2×10^{-3}

(a)   XZ Tau B

3 au

J2000 Declination
J2000 Right Ascension

(b)

Real Visibility (mJy)
(u,v) Distance (Mλ)

ピーク方向の強度分布

観測   モデル

Offset (arcsec)

(b)

Normalized 1.3 mm Continuum Intensity

Offset (AU)

同じアンテナパターンでの
観測予測

(Jy/beam)
0   5×10^{-4} 10^{-3} 1.5×10^{-3} 2×10^{-3}

(d)

3 au

J2000 Right Ascension

A cautionary note about composite Galactic star formation relations

Genevi`eve Parmentier (ApJ)

We explore the pitfalls which affect the comparison of the star formation relation for nearby molecular clouds with that for distant compact molecular clumps. We show that both relations behave differently in the (Σ_{gas}, Σ_{SFR}) space, where Σ_{gas} and Σ_{SFR} are, respectively, the gas and star formation rate surface densities, even when the physics of star formation is the same. This is because the star formation relation of nearby clouds relates gas and star surface densities measured locally, that is, within a given interval of gas surface density, or at a given protostar location. We refer to such measurements as local measurements, and the corresponding star formation relation as the local relation. In contrast, the stellar content of a distant molecular clump remains unresolved. Only the mean star formation rate can be obtained from e.g. the clump infrared luminosity. One clump therefore provides one single point to the (Σ_{gas}, Σ_{SFR}) space, that is, its mean gas surface density and star formation rate surface density. We refer to this star formation relation as a global relation since it builds on the global properties of molecular clumps. Its definition therefore requires an ensemble of cluster-forming clumps. We show that, although the local and global relations have different slopes, this per se cannot be taken as evidence for a change in the physics of star formation with gas surface density. It therefore appears that great caution should be taken when physically interpreting a composite star formation relation, that is, a relation combining together local and global relations.

Kennicutt+Schmidt則

$$\Sigma_{SFR} \propto \Sigma_{gas}^{N} \qquad N \simeq 1.4$$

High density tracer HCN

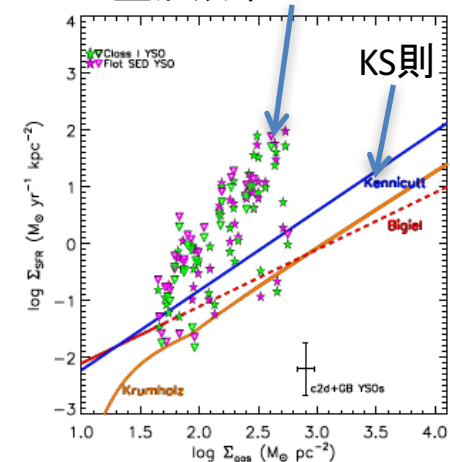$$\Sigma_{IR} \propto \Sigma_{HCN} \qquad \text{Gao+Solomon (2004)}$$

彼らもCOでならN=1.4

localな星形成率とガスの面密度
の関係(pc scale)

$$\Sigma_{*} \propto \Sigma_{gas}^{N'}$$
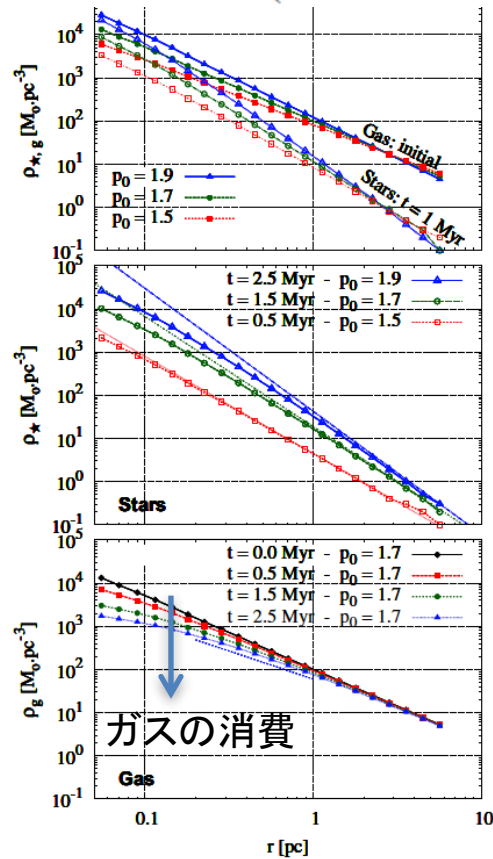$$N' \simeq 2$$

YSOの数から決め
た星形成率

KS則

Heiderman +2010

☆形成

$$\rho_{SFR} \propto \frac{\rho_{gas}}{(G\rho_{gas})^{-1/2}} \propto \rho_{gas}^{1.5}$$

$$\frac{\partial \rho_g(t,r)}{\partial t} = -\frac{\epsilon_{ff}}{\tau_{ff}(t,r)}\rho_g(t,r) = -\sqrt{\frac{32G}{3\pi}}\epsilon_{ff}\rho_g(t,r)^{3/2} \qquad (17)$$

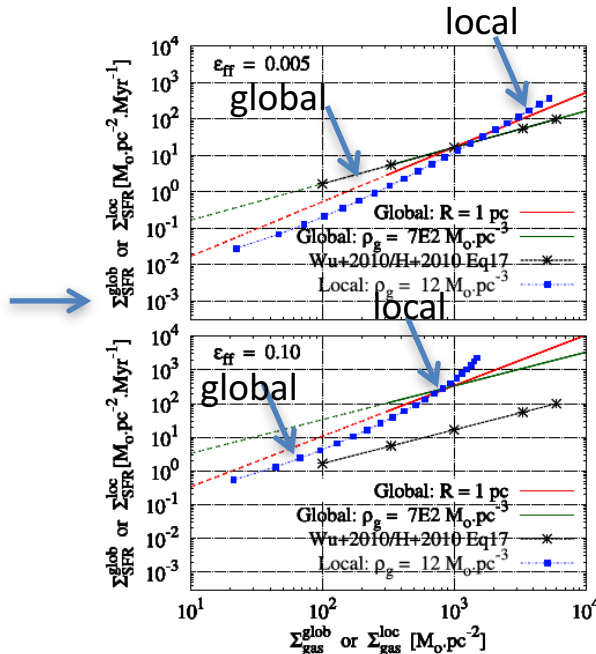$$\frac{\partial \rho_\star(t,r)}{\partial t} = \frac{\epsilon_{ff}}{\tau_{ff}(t,r)}\rho_g(t,r) = \sqrt{\frac{32G}{3\pi}}\epsilon_{ff}\rho_g(t,r)^{3/2}, \qquad (18)$$

$$\rho_g(t,r) = \left(\rho_0(r)^{-1/2} + \sqrt{\frac{8G}{3\pi}}\epsilon_{ff}t\right)^{-2},$$

$$\rho_\star(t,r) = \rho_0(r) - \left(\rho_0(r)^{-1/2} + \sqrt{\frac{8G}{3\pi}}\epsilon_{ff}t\right)^{-2}$$

A. Global Measurement   B. Local Measurements

$$\rho \rightarrow \Sigma$$

ガスの消費

local

global

local

global